Climate Dynamics
https://doi.org/10.1007/s00382-019-04813-1

# Temperature influence on peatland carbon accumulation over the last century in Northeast China

**Hanxiang Liu[1,2] · Zicheng Yu[3,4] · Dongxue Han[1,2] · Chuanyu Gao[1] · Xiaofei Yu[1,4] · Guoping Wang[1]**

Received: 14 December 2018 / Accepted: 8 May 2019
© Springer-Verlag GmbH Germany, part of Springer Nature 2019

## Abstract

Here we present results from a total of 10 peatland cores dated by $^{210}Pb$ analysis in the Greater Khingan Range and Sanjiang Plain, Northeast China to determine their carbon accumulation rates and evaluate possible climate connections during the last 100 years. The carbon accumulation rate and temperature in the Greater Khingan Range were lower than that in the Sanjiang Plain. Carbon accumulation rate in the last 100 years was higher than the long-term rate of carbon accumulation in the last two millennia mainly due to the addition of peat was more obvious than the decomposition on the background of warming. Regression relationships between temperature and Non-autogenic carbon accumulation rate were constructed by GAMs, GBMs, and RF models. We also predicted the trend of carbon accumulation rate in Northeast China over the next century based on these models. The future carbon accumulation rates in the Great Khingan Range under RCP 2.6 and RCP 8.5 will increase until around 2100 CE in the face of warming. Future peatland carbon accumulation rate under a warmer climate show a decrease in the Sanjiang Plain under RCP 2.6 and RCP 8.5.

**Keywords** Carbon accumulation rate · Temperature · Region compare · Regression model · Future change tendency

## 1 Introduction

The rate of photosynthesis, organic matter decomposition, and $CO_2$ and $CH_4$ emissions in peatlands are greatly influenced by climate conditions (Gorham 1991; Stocker et al. 2017). The carbon accumulation rate in peatlands, determined by the balance between net primary production (NPP) and organic decomposition, is the key element in understanding the relationship between global carbon cycle and global change. The temperature measured on land and at sea for more than a century show that Earth's globally averaged surface temperature is rising. It is said that the global surface temperature has increased by ~0.2 °C per decade in the past half-century (Hansen et al. 2006), and an increasing body of observations gives a collective picture of a warming world (Ekwurzel et al. 2017; Hausfather et al. 2017; Karl et al. 2015). The rates of NPP and microbial decomposition will increase with warming, but it remains unclear which dominate the peatland carbon accumulation rate (Gallego-Sala et al. 2018).

Different hydrothermal combinations play different roles in carbon accumulation. It depends on which factor (temperature, hydrology or plant species, etc.) is the crucial limitation factor in the particular site (Straková et al. 2012; Sullivan et al. 2008). Regional studies show different or sometimes opposite conclusions about the effect of temperature and moisture changes on peat C accumulation. For example, the decline in carbon accumulation was caused by relatively dry and warm climate, and the development of cooler and moister climate led to the increase of carbon accumulation in the peatland of Finland (Mäkilä et al. 2001;

**Electronic supplementary material** The online version of this article (https://doi.org/10.1007/s00382-019-04813-1) contains supplementary material, which is available to authorized users.

✉ Xiaofei Yu
yuxf@iga.ac.cn

✉ Guoping Wang
wangguoping@neigae.ac.cn

1 Key Laboratory of Peatland Ecology and Environment, Northeast Institute of Geography and Agroecology, Chinese Academy of Sciences, Changchun 130102, China

2 University of Chinese Academy of Sciences, Beijing 100049, China

3 Department of Earth and Environment Sciences, Lehigh University, Bethlehem, PA 18015, USA

4 Northeast Normal University, Changchun 130024, China

Ukonmaanaho et al. 2006). However, the widespread slowdown of carbon accumulation of fen peatlands had been found by other scientists result from climate cooling (Gao et al. 2010; Klein et al. 2013; Yu 2006). Thus, the role of influence factors on carbon accumulation should be seriously evaluated by regions. Some researchers focused on the new extensive database of peat profiles across northern peatlands to examine spatial and temporal patterns of carbon accumulation over the past millennium. Their results indicated that the carbon sequestration rate could increase over many areas of northern peatlands in a warmer future (Charman et al. 2013; Loisel et al. 2014).

The boreal and subarctic peatlands cover extensive areas of the world's peatlands and represent one of the largest carbon reservoirs in the terrestrial ecosystem (Yu 2012). Some scientists focused on the long-term apparent rate of carbon accumulation (LORCA) to understand the climate change in the Holocene (Gorham 1991; Stelling et al. 2018; Yu et al. 2003a), while other scientists were interested in the recent apparent rate of carbon accumulation (RERCA) with the increasing of carbon emission and the intensity of human activities (Klein et al. 2013; Loisel and Yu 2013b; Ukonmaanaho et al. 2006). The high-latitude area is sensitive to climate change and the carbon accumulation likely to be affected by rising temperature (Davidson et al. 2000). Northeast China located in the typical boreal peatland region, and this region's LORCA and carbon storages during the last two millennia were quantified and estimated by Xing et al. (2015) based on 134 peatland cores. They found that the photosynthetically active radiation over the growing season played a major role in determining the carbon accumulation, but they did not focus on the timescale for recent 100 years. The variations of RERCA and carbon fluxes in the recent 100 years of the peatland in the Sanjiang Plain, Northeast China were estimated by Bao et al. (2011) based on 10 peat cores, as well as the RERCA in Motianling peatland of the Greater Khingan Range based on 3 peat cores (Bao et al., 2015). However, the climate-driven patterns of carbon accumulation were not involved in these studies. Due to the differences in latitude–longitude and elevation, the temperatures are different between the Greater Khingan Range and Sanjiang Plain. The two regions are a good choice for studying the relationship between carbon accumulation and temperature.

Here, we used $^{210}$Pb dating technique to construct the age-depth models of 10 peatland cores (6 in the Greater Khingan Range and 4 in the Sanjiang Plain) and calculate the carbon accumulation rates of each core over the recent 100 years. Our objectives are to (1) compare carbon accumulation between the Greater Khingan Range and Sanjiang Plain, (2) construct regression relationship between carbon accumulation rate and temperature by using statistical models, and (3) predict the trend of carbon accumulation rate in Northeast China over the next century. The study on the relationship between carbon accumulation and temperature will improve understanding of the role of peatlands in climate change and provide a valuable perspective of the future global carbon cycle.

## 2 Materials and methods

### 2.1 Study area and sediment samplings

Northeast China is characterized by a cold temperate continental monsoon climate with a short, warm, wet summer and a long, cold, dry winter. A large number of wetlands developed in this region, and accounting for 48% of the total area of wetlands in China (Niu et al. 2012). The Greater Khingan Range contains the upper tributaries of the Amur River (that is, Heilongjiang River), which forms the border between Northeast China and Russia Far East (Fig. 1), and the Sanjiang Plain locates in the middle reaches of the Amur River. The annual precipitation is 469 mm and the annual temperature is − 4.16 °C based on the arithmetical mean of Tulihe and Huzhong weather stations in the Greater Khingan Range, and the annual precipitation is 520 mm and the annual temperature is 2.75 °C based on the arithmetical mean of Fujin and Tongjiang stations in the Sanjiang Plain. The average elevations of the Greater Khingan Range and Sanjiang Plain are 573 and 50 m, and the annual sunshine durations are 2514 h and 2434 h.

The Wardenaar peat corer (Eijkelkamp, Netherlands) was used to collect peat cores, and the monolith dimensions are 10 cm × 10 cm × 100 cm. A total of 10 cores in 9 peatlands was sampled, 6 in the Greater Khingan Range and 4 in the Sanjiang Plain (Fig. 1 and Table 1). GH, HY and SJD are valley peatlands that their available water mainly sources from precipitation and mountain snow meltwater. PG, TQ, HT, MG, HH and QDL are riparian peatlands that their available water mainly from runoff. Due to there is almost permafrost below the surface 50–100 cm in the Greater Khingan Range, the length of each core is less than 50 cm, and cores were sectioned at 1-cm intervals with a stainless-steel hand saw in the field. The collected samples were packed into polyethylene plastic ziplock bags for transport to the laboratory, and then refrigerated at 4 °C for further analysis.

### 2.2 $^{210}$Pb dating method

Every 1-cm section subsample was ground into powder and filled the 7 ml plastic quasi-cylindrical bottle up. Three weeks after samples stored in sealed plastic bags to balance the radioactivity, the radioactivities of total $^{210}$Pb (46.5 keV), $^{214}$Pb (352 keV) and $^{214}$Bi (609 keV) were measured using

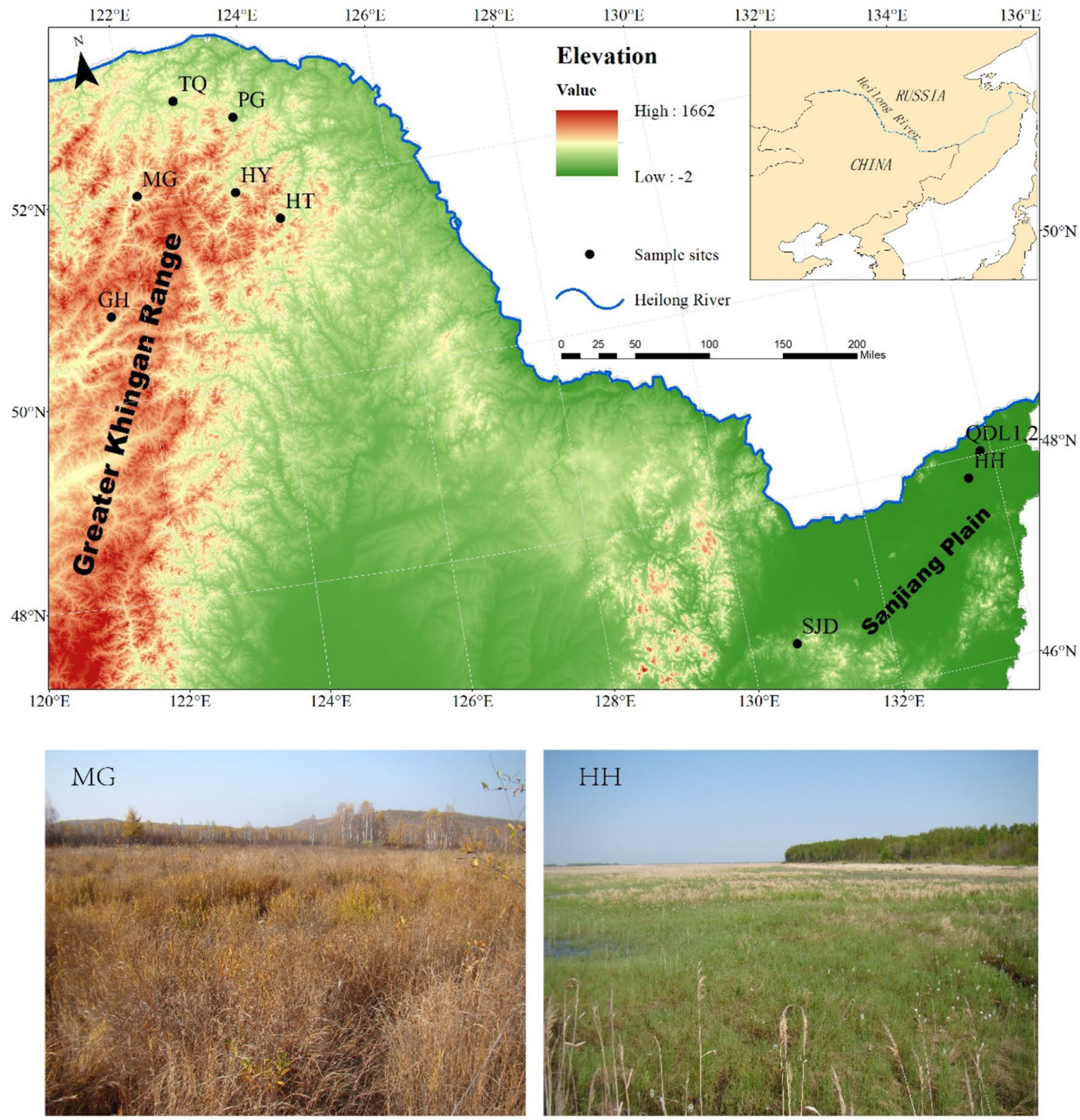


**Fig. 1** Location of the sampling sites and photos of two typical peatlands (Valley peatland and riparian peatland) in the Greater Khingan Range and Sanjiang Plain, Northeast China

low background gamma spectroscopy (ORTEC Instruments Ltd., USA) at the Analysis and Test Center of the Northeast Institute of Geography and Agroecology (IGA) of the Chinese Academy of Sciences (CAS). The counting time was set as 40,000 s to ensure the measurement precision. $^{226}$Ra radioactivity was calculated from the means of $^{214}$Pb and $^{214}$Bi (Van Cleef 1994), and $^{226}$Ra radioactivity is considered to reflect the supported $^{210}$Pb. The standard radioactive sources of know activities and reference dates were supplied by the National Institute of Metrology in China ($^{210}$Pb: 1.39e + 02 Bq, 2016-06-08; $^{226}$Ra: 3.83E + 01 Bq, 2016-06-05). The age-depth framework was constructed by applying the constant rate of supply (CRS) model based on the unsupported $^{210}$Pb radioactivity (Appleby and Oldfield 1978). The CRS model is to assume that the supply of unsupported $^{210}$Pb to the sediment is the same for each time interval, and the time can be calculated using the radioactivity and half-life of unsupported $^{210}$Pb.

## 2.3 Sediment properties analysis

Volumetric subsamples of 17 ml were taken using an aluminum specimen box and were dried at 105 °C for 12 h to determine dry bulk density (DBD), the ratio of dry weight to volume is DBD. A portion of dried subsamples was combusted at 550 °C in a muffle furnace for 4 h to measure loss

**Table 1** Detailed information about the sampling cores in Northeast China

| Sampling Cores | Location | Elevation (m) | Dated Depth/Year (cm CE$^{-1}$) | Peatland type | Mean OC (%) | Mean DBD (g cm$^{-3}$) | PAR (g m$^{-2}$year$^{-1}$) | Decay coefficient (year$^{-1}$) |
|---|---|---|---|---|---|---|---|---|
| Pangu (PG) | 123.7450E, 52.7026N | 495 | 32/1906 ± 4 | Riparian peatland | 48 ± 1 | 0.09 ± 0.04 | 505 | 0.017 |
| Huyuan (HY) | 123.6317E, 51.9445N | 575 | 32/1901 ± 6 | Valley peatland | 37 ± 4 | 0.13 ± 0.04 | 300 | 0.0006 |
| Mangui (MG) | 122.1227E, 52.0255N | 650 | 28/1911 ± 2 | Riparian peatland | 33 ± 7 | 0.20 ± 0.12 | 367 | 0.0001 |
| Genhe (GH) | 121.5058E, 50.8612N | 776 | 27/1913 ± 4 | Valley peatland | 30 ± 7 | 0.20 ± 0.05 | 229 | 0.0008 |
| Tuqiang (TQ) | 122.8549E, 52.9429N | 475 | 29/1908 ± 2 | Riparian peatland | 37 ± 6 | 0.14 ± 0.04 | 470 | 0.01 |
| Hongtu (HT) | 124.2405E, 51.6190N | 552 | 36/1901 ± 8 | Riparian peatland | 43 ± 2 | 0.07 ± 0.02 | 264 | 0.005 |
| Honghe (HH2) | 133.6275E, 47.7886N | 50 | 46/1901 ± 1 | Riparian peatland | 40 ± 3 | 0.15 ± 0.02 | 737 | 0.012 |
| Qindeli1 (QDL1) | 133.3431E, 48.0347 N | 56 | 26/1910 ± 4 | Riparian peatland | 37 ± 3 | 0.19 ± 0.02 | 644 | 0.013 |
| Qindeli2 (QDL2) | 133.3424E, 48.0350N | 57 | 32/1910 ± 1 | Riparian peatland | 36 ± 2 | 0.18 ± 0.02 | 752 | 0.009 |
| Shenjiadian (SJD) | 130.6644E, 46.5811N | 155 | 30/1912 ± 2 | Valley peatland | 30 ± 3 | 0.28 ± 0.03 | 926 | 0.012 |

The first 6 peat cores are from the Greater Khingan Range, and the following 4 peat cores are from the Sanjiang Plain

on ignition (LOI) as an estimate of organic matter content (Beilman et al. 2009). The organic carbon content (OC) were determined by multiplying the organic matter content by 50% (Chambers et al. 2011; Loisel et al. 2014).

## 2.4 Calculation of carbon accumulation and decomposition

Based on the age-depth models and the measured DBD (g cm$^{-3}$) and OC (%), the RERCA (g cm$^{-2}$ year$^{-1}$) was calculated according to the following equation (Tolonen and Turunen 1996):

$$RERCA = r \times DBD \times OC \times 100, \quad (1)$$

where $r$ is the rate of peat height increment (cm year$^{-1}$). Assuming a constant peat addition rate (PAR, g cm$^{-2}$ year$^{-1}$) at the top of the peat column, and a constant peat decay coefficient (α), the exponential decay model derived from Clymo (1984):

$$X = \frac{PAR}{\alpha} \times \left(1 - e^{-\alpha t}\right), \quad (2)$$

is used to represent recent peat decomposition, where $X$ is cumulative peat (g cm$^{-2}$) in a certain period (*t, yr*). The PAR determines the general slope of the cumulative peat versus age curve, and the α determines the curvature of the curve (Yu et al. 2000, 2003b). The PAR and α of each peat core were evaluated through curve fitting exercise produces. The bottom layer has more decomposition time than the upper layer due to the autogenic process in peat accumulation. Decay models were fit individually to each carbon accumulation curve, then the changes in carbon accumulation rates (Non-autogenic CAR) for each site were expressed as differences between apparent accumulation and those derived from the Clymo's model (Charman et al. 2013). Negative value represents decomposition greater than accumulation. To avoid biases in the calculation of carbon accumulation rate, the Non-autogenic CAR of each peatland core was estimated by taking the 5-year moving average with 1-year interval interpolation. Finally, two time series of Non-autogenic CAR of the Greater Khingan Range and Sanjiang Plain were calculated as the median of the 10 interpolated accumulation rates (each peat core).

The carbon storages of the recent 100 years in the peatlands of the Greater Khingan Range and Sanjiang Plain were estimated based on the carbon density approach which is one of the common methods used for estimating the carbon pool (Yu 2012). The equation is:

$$C\,storage(Gt) = A \times h \times DBD \times OC \times 10^{-5}, \quad (3)$$

where $Gt$ is Giga ton, A is peatland area (km$^2$), $h$ is peat depth (cm), $DBD \times OC$ is the carbon density (g C cm$^{-3}$). The mean peat depth and carbon density values of the peat cores were used to evaluate the carbon storages in the two regions.

### 2.5 Regression models and prediction

Regression models were used to construct the relationship between Non-autogenic CAR and temperature, and to predict the potential changes of Non-autogenic CAR under future climate patterns in the Northeast China. These models included Generalized Additive Models (GAMs) (Hastie and Tibshirani 1986), Generalized Boosting Models (GBMs) (Ridgeway 2007) and Random Forest (RF) (Breiman 2001). The choice of the smoothing parameters was made through generalized cross-validation method, and the residual was assumed to be a Gaussian distribution. The GAMs of Non-autogenic CAR and temperature (annual temperature, summer temperature and winter temperature) were constructed respectively to determine the final model based on the lowest Akaike information criterion (AIC). The final model's temperature and Non-autogenic CAR datasets were added to the other models using the *gbm* and *randomForest* functions in the R environment.

The temperature changes of Greater Khingan Range and Sanjiang Plain in the future 100 years were predicted based on the combined materials of Amon_MIROC5 model in CMIP5 (Coupled Model Inter-comparison Project Phase 5) under different representative concentration pathways (RCPs). The Amon_MIROC5 model performs better than the majority (50%) of all the models in CMIP5 in Northeast China (Ao et al. 2017; Wang et al. 2017). Based on the climate change data of the Greater Khingan Range and Sanjiang Plain in the future 100 years, the future change tendency of carbon accumulation rate was predicted using the *predict* function and regression models.

## 3 Results

### 3.1 Chronologies

The unsupported $^{210}$Pb activities are shown in Fig. S1 (Supplementary Figures) and the age-depth frameworks are shown in Fig. 2. In order to unify the length of time in peat cores, only the years after 1900 CE (Common Era) were

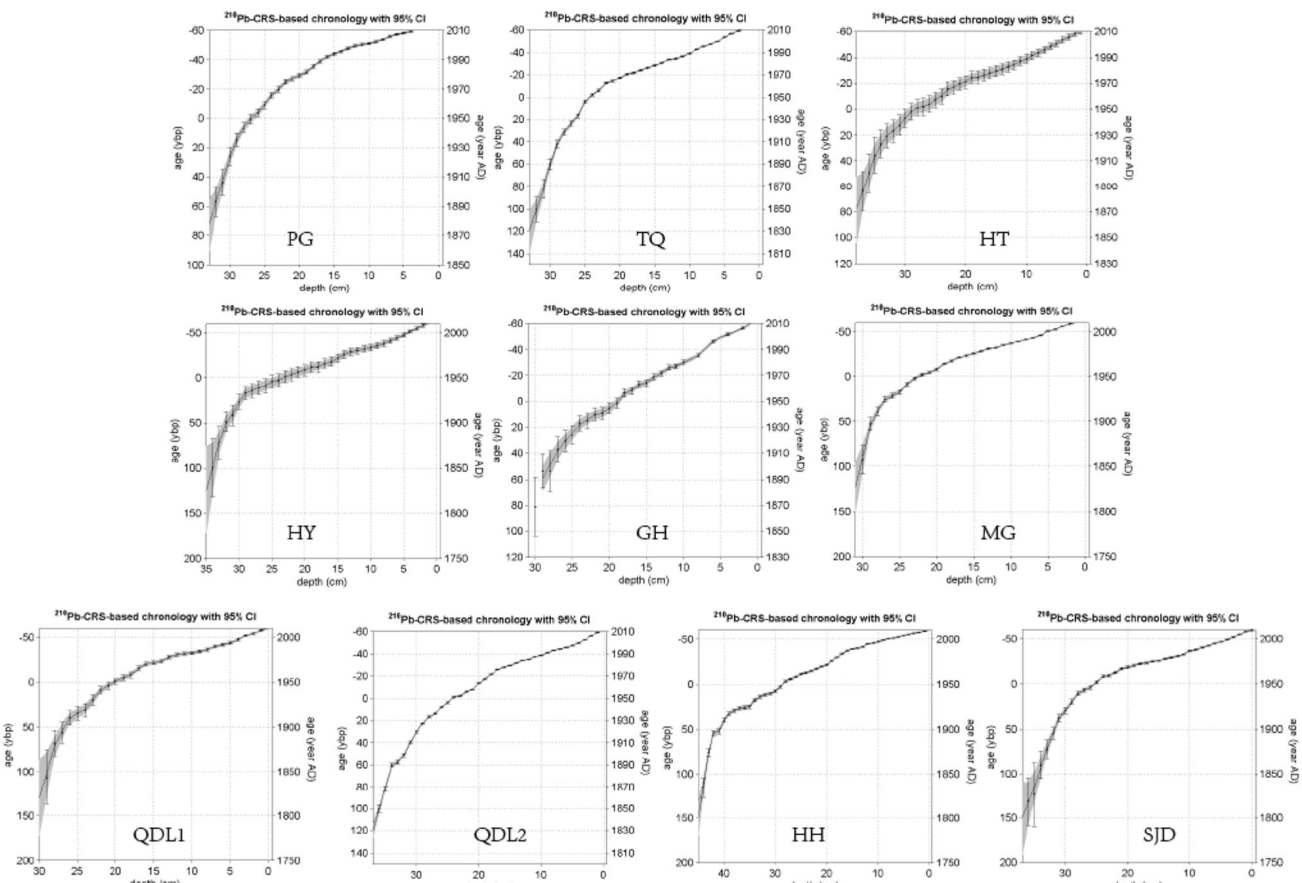


**Fig. 2** The age-depth models of peat cores in the Greater Khingan Range and Sanjiang Plain. The definitions of all acronyms are shown in Table 1

used. The dated depth of HH was the longest (46 cm), with the bottom year of 1901 ± 1 CE, while QDL1 was the shortest (26 cm), with the bottom year of 1910 ± 4 CE (Table 1).

### 3.2 Dry bulk density and organic carbon

DBD of peat cores ranged from 0.04 to 1.48 g $cm^{-3}$, the highest value occurred in SJD (mean and standard deviation: 0.28 ± 0.03 g $cm^{-3}$) and the lowest appeared in HT (mean: 0.07 ± 0.02 g $cm^{-3}$). The ranges of OC were 30–48% that PG had the highest mean value (48 ± 1%) and GH had the lowest mean value (30 ± 7%) (Table 1). The DBD of TQ, PG, MG, HY, HH, and QDL2 all had increasing trends with depth, and OC values change in the opposite trends. But the DBD of HT and GH showed a wavelike decrease, the DBD and OC of QDL2 and SJD were stable (Fig. S2).

### 3.3 Recent carbon dynamics

The cumulative peat ranged from 203 to 341 g $cm^{-2}$ over the last 100 years in the peatlands of the Greater Khingan Range, and from 407 to 747 g $cm^{-2}$ in the peatlands of the Sanjing Plain. PAR ranged from 229 to 505 g $m^{-2}$ $year^{-1}$ in the Greater Khingan Range, and 644-926 g $m^{-2}$ $year^{-1}$ in the Sanjing Plain. The mean values of PAR were 356 and 765 g $m^{-2}$ $year^{-1}$ in the Greater Khingan Range and Sanjing Plain. Decay coefficients (α) ranged from 0.0001 to 0.017 $year^{-1}$, with a mean value of 0.0056 $year^{-1}$ in the Greater Khingan Range. The data of the peatlands in the Sanjiang Plain showed higher values for decay coefficients, with a mean α of 0.012 $year^{-1}$, ranging from 0.009 to 0.013 $year^{-1}$ (Fig. 3).

The variations of RERCA and Non-autogenic CAR in each peat core can be seen in Fig. S3. RERCA for all peatland cores ranged from 22 to 1056 g C $m^{-2}$ $year^{-1}$, while Non-autogenic CAR of these cores ranged from − 209 to 726 g C $m^{-2}$ $year^{-1}$. There were RERCA and Non-autogenic CAR peaks around the 1980s and 1950s in almost all peat cores. Based on the average Non-autogenic CAR of TQ, PG, HT, HY, MG and GH, the estimated Non-autogenic CAR of the Greater Khingan Range was 38 ± 26 g C $m^{-2}$ $year^{-1}$. The estimated Non-autogenic CAR of the Sanjiang Plain was 61 ± 11 g C $m^{-2}$ $year^{-1}$ according to the average of HH, QDL1, QDL2 and SJD (Fig. 4). The Non-autogenic CAR values increased from the late 1910s to the late 1960s in the Greater Khingan Range, after that, the Non-autogenic CAR showed a decreasing trend from the 1960s to the present. The Non-autogenic CAR in the Sanjiang Plain almost showed an increasing trend from the 1930s to 1990s. The Non-autogenic CAR peaks of Greater Khingan Range and Sanjiang Plain were occurred from the 1960s (Fig. 5).

Based on the average values of depth, DBD and OC in the peatlands during the recent 100 years, the mean depths of the Greater Khingan Range and Sanjiang Plain were estimated to be 31 and 34 cm, the mean carbon density in the Greater Khingan Range is 0.05 g C $cm^{-3}$, and the Sanjiang Plain is 0.09 g C $cm^{-3}$. The natural peatland areas in the Greater Khingan Range and Sanjiang Plain are 42,450 and 10,520 $km^2$, according to the results of the second National Wetland Resources Survey 2009–2013 (State

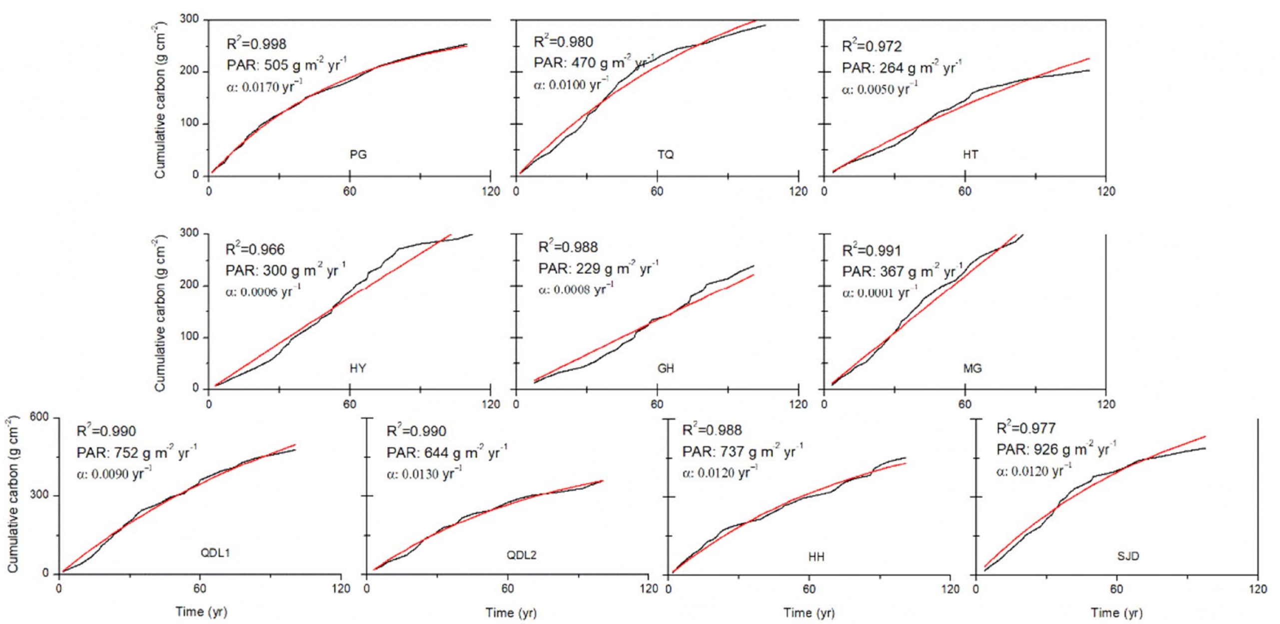


**Fig. 3** The cumulative peat and exponential decay modeling results of the peatland cores in the Greater Khingan Range and Sanjiang Plain. The red lines represent the fitted models

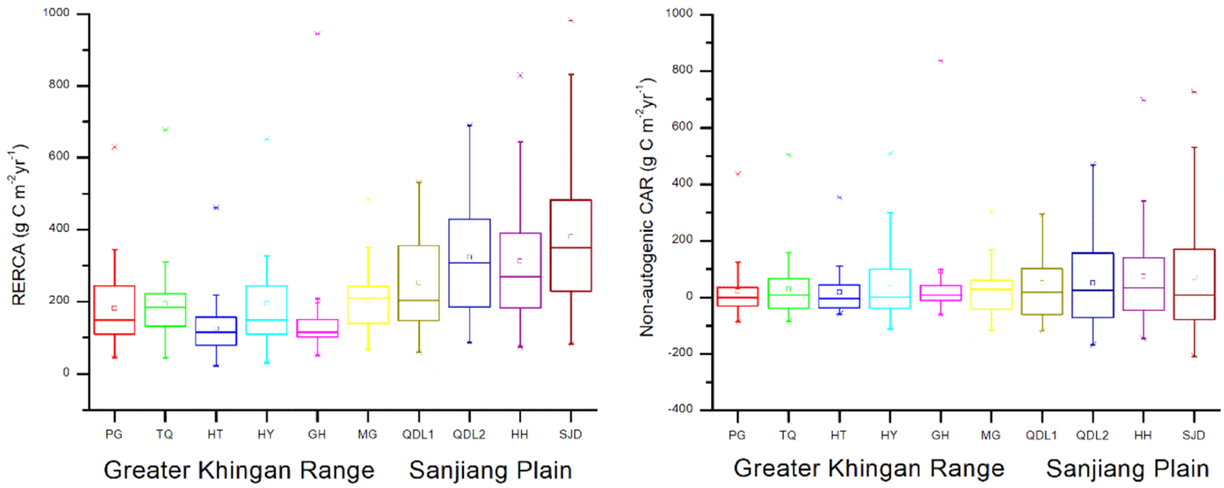


**Fig. 4** Box–Whisker plots of recent apparent carbon accumulation rate (RERCA, left) and Non-autogenic carbon accumulation rate (Non-autogenic CAR, right) of the peatland cores in the Greater Khingan Range and Sanjiang Plain. square: mean values, diamond: max and min values

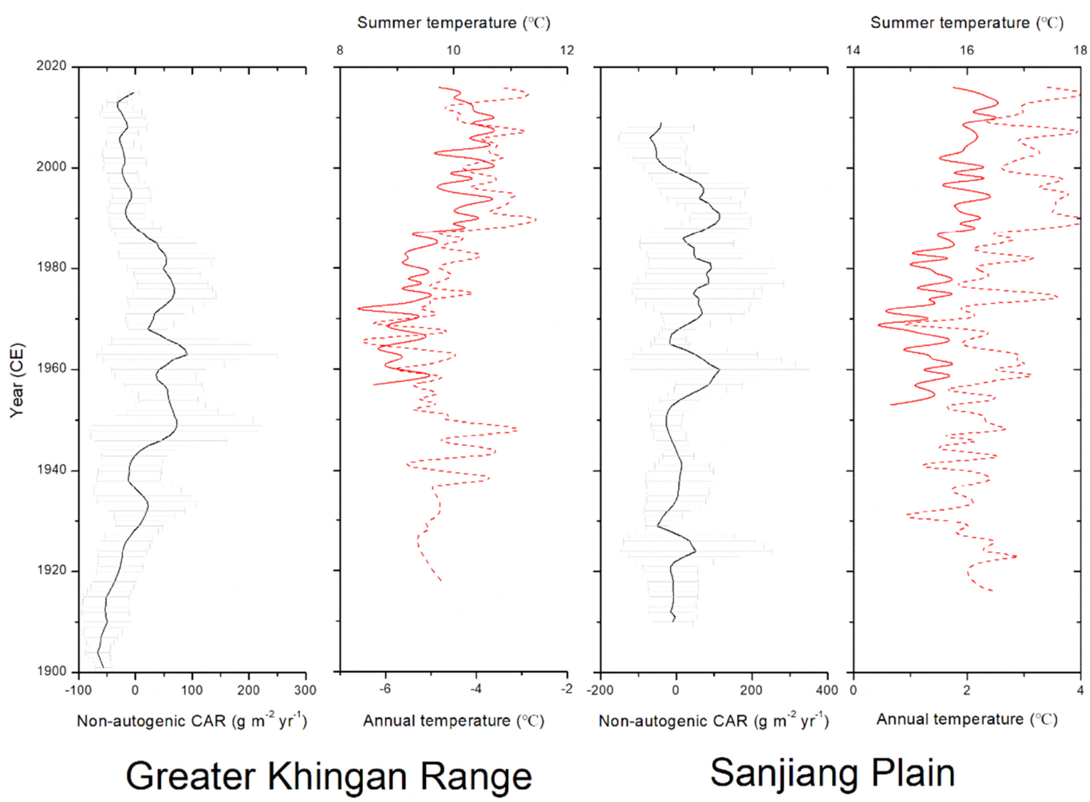


**Fig. 5** The Non-autogenic carbon accumulation rate and meteorological data of the Greater Khingan Range and Sanjiang Plain. The dark lines represent Non-autogenic carbon accumulation rate values, light grey lines represent their standard deviations, red solid and dash lines respectively represent the summer temperature and annual temperature

Forestry Administration 2014). The total carbon storages of the Greater Khingan Range and Sanjiang Plain are 0.66 ($42{,}450 \times 0.05 \times 31 \times 10^{-5}$) and 0.32 Gt C ($10{,}520 \times 0.09 \times 34 \times 10^{-5}$) based on Eq. (3) during the recent 100 years.

### 3.4 Models of carbon accumulation rate and temperature

The AICs of GAMs: $\log(CAR) = s(tem)$, $\log(CAR) = s(sumtem)$ and $\log(CAR) = s(wintem)$ were 1206, 1196 and 1219, respectively. Thus, the final GAM is $\log(CAR) = s(sumtem)$, and this model explained 74.8% of the variance of the Non-autogenic CAR. The summer temperature ($F=6.396$, $df=5.253$, $P<0.001$) and annual temperature ($F=3.803$, $df=6.162$, $P<0.01$) were significant meteorological parameters for Non-autogenic CAR. Area Under the Curve (AUC) were used to measure model accuracy. Useful models produce AUC values above 0.7 usually. Compared with the GAMs (0.855), the GBMs had lower AUC values (0.764), and the RadomForest also performed well with higher AUC values (0.937).

The variations of predicted carbon accumulation rate in the coming century are showed in Fig. 7. Mean value of the predicted carbon accumulation rate of the three models is approximately $8.96 \pm 3.58$ g C $m^{-2}$ $year^{-1}$ under RCP 8.5 in the Greater Khingan Range, the mean values are $-2.49 \pm 1.26$ and $31.39 \pm 1.11$ g C $m^{-2}$ $year^{-1}$ respectively under RCP 2.6 and RCP 4.5. The mean value of the three models is approximately $26.89 \pm 4.06$ g C $m^{-2}$ $year^{-1}$ under RCP 8.5 in the Sanjiang Plain, and the carbon accumulation rate are $29.81 \pm 1.19$ and $18.06 \pm 3.15$ g C $m^{-2}$ $year^{-1}$ under RCP 2.6 and RCP 4.5.

## 4 Discussions

### 4.1 Spatial patterns of recent carbon accumulation

PAR values as derived from the Clymo-type model represent long-term litter input to the acrotelm (the surface oxic layer above the permanent water table) and plant production of peatlands, and PAR can be seen as the main control for peat height (Loisel and Yu 2013a). The PAR in the peatlands of the Sanjiang Plain were all higher than that in the Greater Khingan Range. Even the minimum PAR value in the Sanjiang Plain was greater than the highest PAR value in the Greater Khingan Range (Fig. 3). Comparing the climate conditions which could influence the PAR and decomposition in the two regions, the annual precipitation of Sanjiang Plain is almost similar with the Greater Khingan Range, and the annual temperature of Sanjiang Plain is near 7 °C higher than the Greater Khingan Range (Fig. 5), but the annual sunshine duration of the Sanjiang Plain (2434 h) is a little shorter than the Greater Khingan Range (2514 h) according to the meteorological data. It seems to be possible that the difference of PAR between the two regions was driven by temperature. As the previous studies concluded, the PAR, just like the NPP is dependent on a number of environmental conditions (precipitation, temperature and sunshine duration etc.), and the first in order among these are temperature and available water (Lieth 1975). The plant growth in northern middle and high latitudes has mainly enhanced by recent climate changes (temperature and $CO_2$) based on both climatic data and satellite observations of vegetation activity from 1982 to 1999 (Dong et al. 2016; Nemani et al. 2003). Many previous studies showed that the low annual temperature in Northeast China is one of the most important limiting factors to the vegetation growth (Fang et al. 2003; Mao et al. 2012). What's more, once the temperature increases, it will facilitate the melting of snow and ice, benefit the advance and extension of the growing season (Song et al. 2017). Dynamics of air temperature resulted in a higher plant carbon uptake, strengthening the regional peat accumulation during the last century. As a result, the NPP or PAR in the peatlands of the Sanjiang Plain were higher than the Greater Khingan Range.

Plant decomposition is controlled by climate, litter quality and nature, an abundance of the decomposing organisms (Coulson and Butterfield 1978; Hobbie 1996; Laiho 2006), and so on. Previous study shown that climate is the dominant factor in areas subjected to unfavorable weather conditions (wet and cold), whereas litter quality largely prevails as the regulator under favorable conditions (dry and warm) (Couˆteaux et al. 1995). Therefore, the plant decomposition of the peatlands was mainly controlled by climate in the Greater Khingan Range and Sanjiang Plain which have cold and wet weather conditions. The decay coefficients (α) of the peatlands in Sanjiang Plain were higher than that in Greater Khingan Range, except PG and TQ. As the decomposition coefficients of PG and TQ were almost similar with the peat cores in the Sanjiang Plain, the increase of decomposition coefficient driven by temperature were not so much obviously.

The RERCA and Non-autogenic CAR in the peatlands of Sanjiang Plain were higher than the Greater Khingan Range (Fig. 4), so the carbon density is. Although the peatland area of the Sanjiang Plain is less than 1/4 of the Greater Khingan Range, the carbon storage in the Sanjiang Plain (0.32 Gt) is about 1/2 of the Greater Khingan Range (0.66 Gt). The spatial differences of PAR, decomposition coefficient (α), RERCA and carbon storage all corresponding to the temperature which is the most significant climate differences between Greater Khingan Range and Sanjiang Plain. That is, higher temperature promotes the increase of NPP or PAR and decomposition coefficient, and the increment of PAR is more obvious than the decomposition rate. This type of situation leads to high carbon accumulation and carbon density, which plays a major role in the carbon storage of peatland.

### 4.2 Temporal variations of recent carbon accumulation

The temporal variations of carbon accumulation confirmed the importance of temperature (Fig. 5). Due to the history of meteorological observations is short in Northeast China (Tulihe, Huzhong, Fujin and Tongjiang weather stations: from the 1950s), we combined the meteorological records of Russian Far East (National Oceanic and Atmospheric Administration databases, http://www.ncdc.noaa.gov) with Northeast China and found their tendencies were almost similar. Therefore, the temperature and precipitation data from the 1900s to 1940s were chosen from the Russian Far East, and from the 1950s to the present were chosen from the Greater Khingan Range and Sanjiang Plain (Fig. S4).

The temperature had a dynamically increasing trend from the late 1920s to 1950s, the Non-autogenic CAR had also increased from the late 1910s to the late 1950s in the Greater Khingan Range. After that, the temperature showed decreasing trend in the period of 1950–1970 CE, and the Non-autogenic CAR was high and stable. The temperature continued to increase from the 1970s to the early 2010s along with the decreased Non-autogenic CAR from the 1980s to the present. It seems that the Non-autogenic CAR change with temperature except the period from the late 1980s. The temperature in the Sanjiang Plain almost showed an increasing trend from the 1930s to 1990s, so did the Non-autogenic CAR. Taken the Greater Khingan Range and Sanjiang Plain as a whole region, there was a positive correlation between Non-autogenic CAR and temperature ($r^2 = 0.65$, $p < 0.01$), but the relationship is nonlinear.

The RERCA and temperature of recent 100 years in both regions were also higher than the carbon accumulation rate and temperature of the last 2000 years. The global mean temperature reconstructions show good agreement during the last two millennia based on the many different published reconstructions of temperature changes, which the temperature increased fast from the last century (Christiansen and Charpentier Ljungqvist 2012; Ljungqvist 2010; Mann and Jones 2003). There was also a warm stage in China since 1920 CE according to the general characteristics of temperature reconstructions (Yang et al., 2002). In consideration of the possible carbon losses from deep peat layers by long-term decomposition, the average LORCA values of the Sanjiang Plain and the Greater Khingan Range were 26.2 g C $m^{-2}$ $year^{-1}$ and 42.7 g C $m^{-2}$ $year^{-1}$ in the last 2000 years (Xing et al. 2015). The RERCA in the Sanjiang Plain was $376 \pm 78$ g C $m^{-2}$ $year^{-1}$, and the Greater Khingan Range was $184 \pm 27$ g C $m^{-2}$ $year^{-1}$ in the recent 100 years. That is to say, the recent carbon accumulation rate was larger than the last two millennia before decomposition in northeast China. Xing et al. (2015) estimated the long-term total carbon storages in peatlands of the Greater Khingan Range and Sanjiang Plain were 2.19 and 0.73 Gt C using an average peat depth of 75–100 cm. As the total carbon storages of the Greater Khingan Range and Sanjiang Plain are 0.66 and 0.32 Gt C in the recent 100 years, compared with the long-term carbon pool (the last two millennia), the recent carbon storages account for 30% and 44%, that is, there was a sharp increase in carbon storage in the recent 100 years. As a background value, the boreal and arctic peatlands have accumulated 400–500 Gt C by assuming an average depth of 2–3 m, and up to about one-third of the world's soil carbon (Gorham 1991; Maltby and Immirzi 1993). The peatlands in the Northeast China are typically boreal peatlands and play their role in the global carbon pool and the carbon cycle.

### 4.3 Future change-tendency of carbon accumulation in Northeast China

Temperature highly determined the spatial difference and temporal variation of carbon accumulation rate in the peatlands of Northeast China by influencing the growth and decomposition of peatland plants. The Non-autogenic CAR of the Greater Khingan Range and Sanjiang Plain were linked to their corresponding temperature using GAMs, GBMs, and RF, and all models passed the significance tests (Fig. 6). The models all showed negative relationships between Non-autogenic CAR and summer temperature in the range of 9 through 10 °C, the increased CAR being associated with the increasing temperature when the annual temperature was higher than 10 °C till 16 °C.

The summer temperature of Greater Khingan Range and Sanjiang Plain in the future 100 years have significant increasing trends under all RCP scenarios. The temperature under RCP 4.5 higher than RCP 2.6 and RCP 8.5 in the Greater Khingan Range, and temperature under RCP 2.6 and RCP 8.5 higher than RCP 4.5 in the Sanjiang Plain. Based on the variations of temperature change and three regression models, we predicted the future change-tendency of carbon accumulation rate by the end of the twenty-first century (Fig. 7). The carbon accumulation rate fluctuate violently around $31.39 \pm 1.11$ g C $m^{-2}$ $year^{-1}$ under RCP 4.5 in the Great Khingan Range based on the three models. The carbon accumulation rates have obvious increasing trends under RCP 2.6 and RCP 8.5 due to the future temperatures have increasing trends and will up to 10 °C. The future carbon accumulation rates in the Great Khingan Range have strong agreement with the global carbon accumulation derived by Gallego-Sala et al. (2018) under RCP 2.6 and RCP 8.5 until around 2100 CE in the face of warming. The future carbon accumulation rate will increase from 2010 to 2090 under RCP 4.5 based on all models. However, the future carbon accumulation rates in Sanjiang Plain decreasing under RCP 2.6 and RCP 8.5, because of the future temperature of Sanjiang Plain is above 16 °C. Modelled changes in the

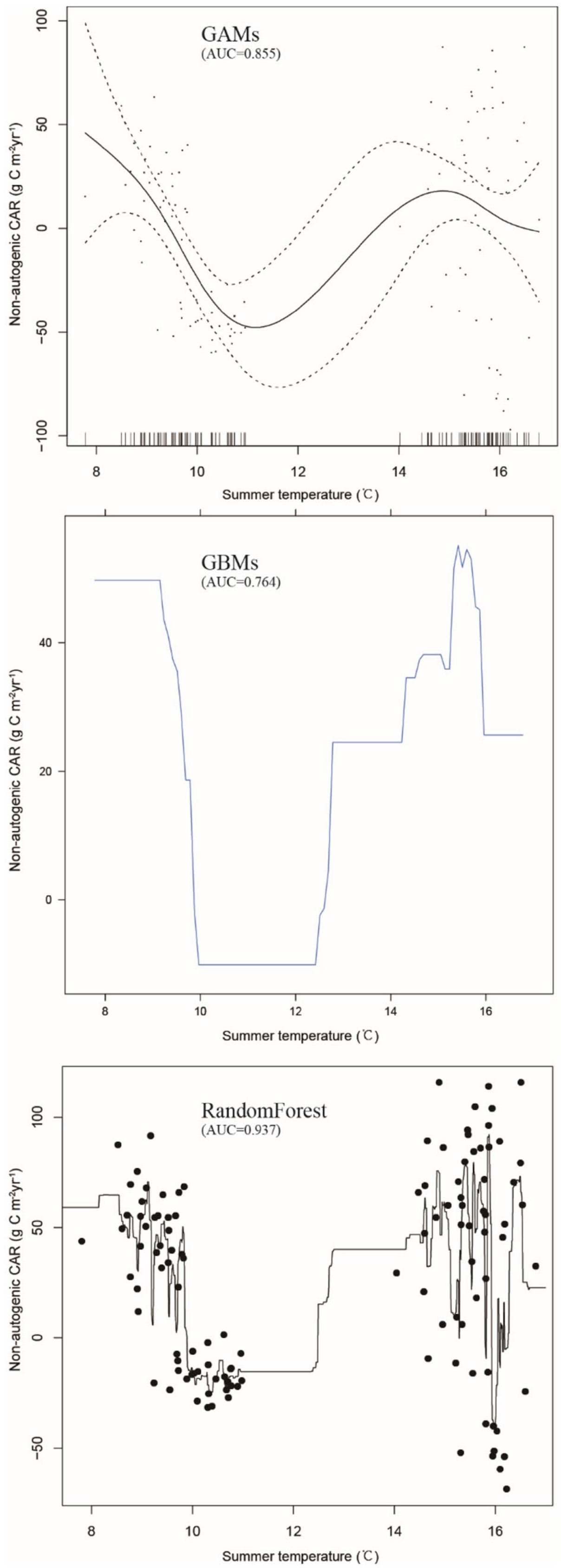


**Fig. 6** The regression models of Non-autogenic carbon accumulation rate and summer temperature

future peatland carbon sink under a warmer climate show a decrease in the Sanjiang Plain. An explanation for the mechanism of change in carbon accumulation is that respiratory losses are rising faster than net primary productivity when the summer temperature is around above 16 °C.

The Greater Khingan Range and Sanjiang Plain have an extensive area of peatland and play an important role in the global carbon cycle. However, due to the fragility and sensitivity of peatland, carbon accumulation rate and storage are highly vulnerable to climate change or human activities. The rapid population growth and land-use across the whole of the Northeast China region have resulted in the conversion of large areas of lowland peatland to agriculture in recent decades (Liu et al. 2018). Peatland drainage for the reclaim or peatland degradation results in the loss of soil organic carbon and releasing additional greenhouse gases to the atmosphere. Human activities and the climate warming make the peatland release the $CO_2$/$CH_4$ to the atmosphere, climate warming could be strengthened by the released greenhouse gases. The peatland carbon accumulation will increase, and the consequent loss of carbon through decomposition of organic matter will continue (Fig. 8). The good news is that the environmental protection policies have initial effects and the reclamation of peatland is almost stopped in Northeast China. The area of farmland stabilized around 158,500 $km^2$ in the Heilongjiang Province since 2009 CE (Statistical Yearbook of Heilongjiang Province), so the peatland area in Northeast China would be stable in the future. Therefore, consider only natural factors, the prediction of future carbon accumulation will be credible.

## 5 Conclusions

Our study provides baseline data on carbon accumulation rate for nearly 100 years in the Greater Khingan Range and the Sanjiang Plain, which were higher than LORCA of the last two millennia. Compared with the last two-millennium carbon pools in the Greater Khingan Range (2.19 Gt C) and the Sanjiang Plain (0.73 Gt C), the last century recent carbon storages in the two regions account for 30% (0.66 Gt C) and 44% (0.32 Gt C). The carbon accumulation rates of the peatlands in Sanjiang Plain were higher than the Greater Khingan Range. The spatial and temporal differences of carbon accumulation in Northeast China were driven by temperature, and the increment of PAR is more obvious than the decomposition coefficient. Regression relationships between CAR and temperature were constructed by the GAMs, GBMs and RF models. Models also predicted carbon accumulation rate by the end of the twenty-first century under three RCP scenarios. The models all showed negative relationships between Non-autogenic CAR and summer temperature in the range of 9 through 10 °C, the increased

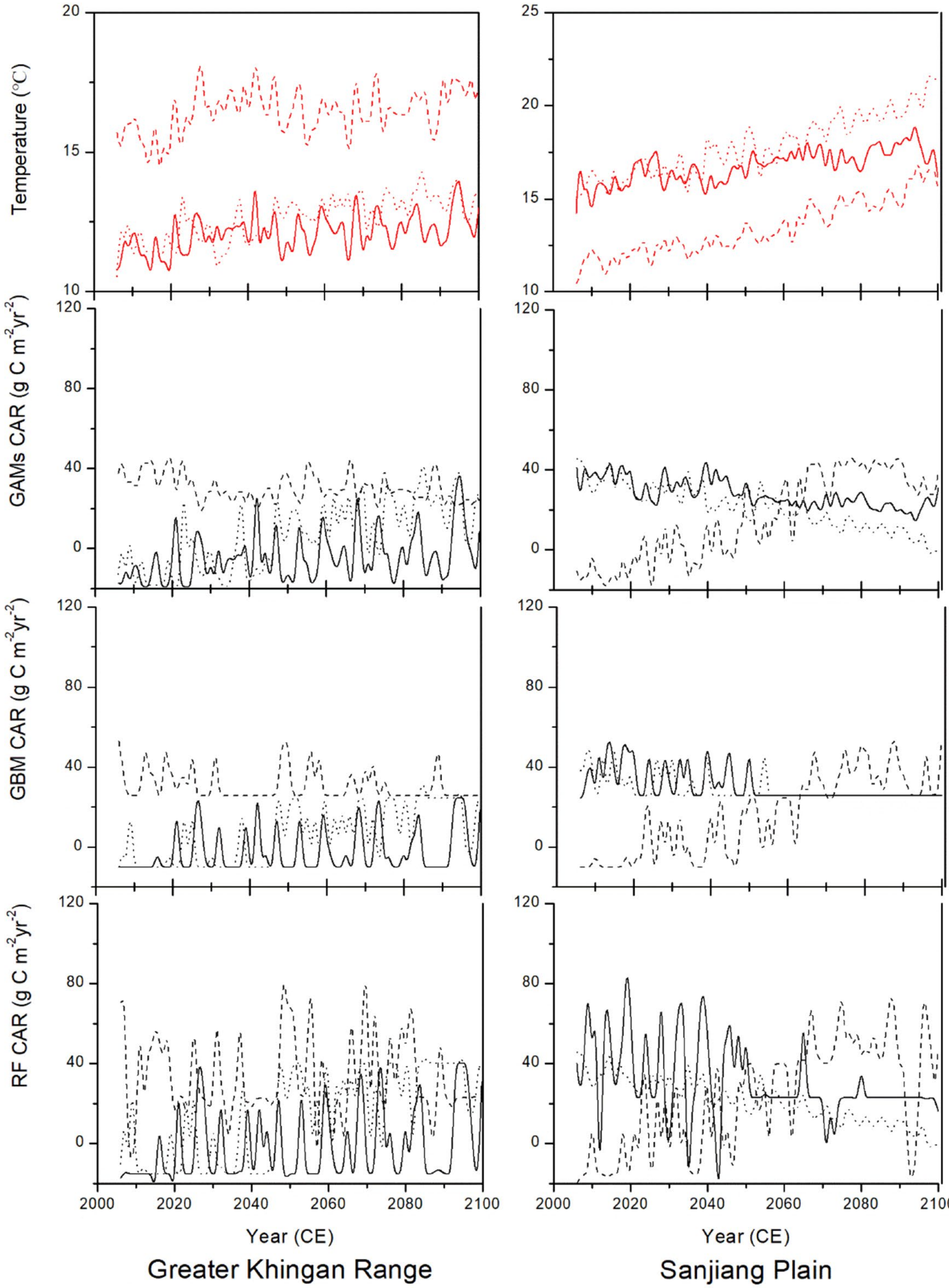


**Fig. 7** Future change-tendency of summer temperature and carbon accumulation rate in the Greater Khingan Range and Sanjiang Plain based on the multi-models in CMIP5. The solid lines represent RCP 2.6, dash lines represent RCP 4.5, and dot lines represent RCP 8.5

CAR being associated with the increasing temperature when the annual temperature was higher than 10 °C till 16 °C. The future carbon accumulation rates in the Great Khingan Range under RCP 2.6 and RCP 8.5 will increase until around 2100 CE in the face of warming. Modelled changes in the future peatland carbon accumulation rate under a warmer

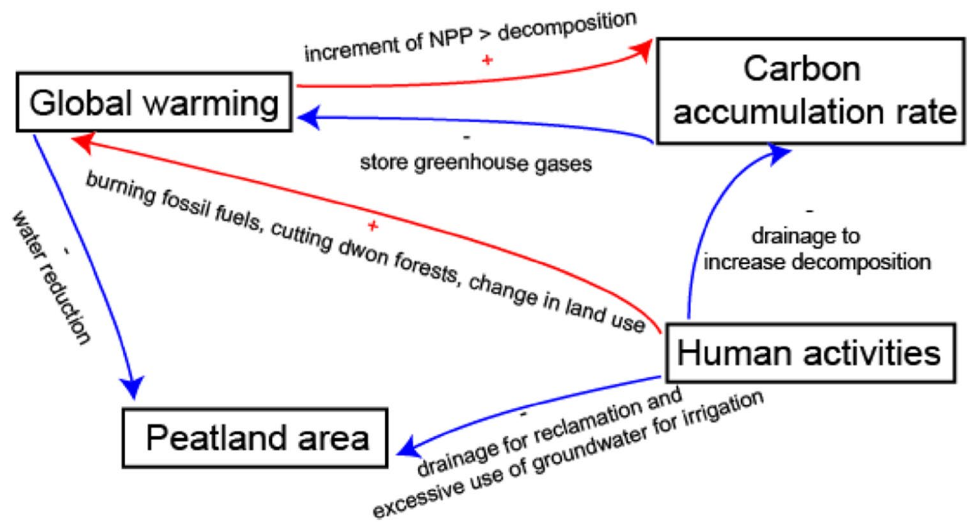


**Fig. 8** A conceptual model of the ongoing global warming and peatland carbon accumulation in the Greater Khingan Range and Sanjiang Plain. The arrows represent processes and the boxes represent variables. The symbols '+' with red indicate positive effect, the symbols '–' with dark blue indicate a negative effect

climate show a decrease in the Sanjiang Plain under RCP 2.6 and RCP 8.5.

**Acknowledgements** The authors gratefully acknowledge the assistance of the Analysis and Test Center, Northeast Institute of Geography and Agroecology, Chinese Academy of Sciences. This work was supported by the National Natural Science Foundation of China (No. 41,571,191, 41701217); and the national key research and development project (No. 2016YFA0602301).

**Conflict of interest** The authors declare that they have no competing interest.

## References

Ao X, Zhai Q, Cui Y, Zhou X, Zhao C (2017) The projections of climate change in Northeast China using CMIP5 models. Meteorol Sci Technol 45:298–306

Appleby PG, Oldfield F (1978) The calculation of lead-210 dates assuming a constant rate of supply of unsupported 210Pb to the sediment. CATENA 5:1–8

Bao K, Zhao H, Xing W, Lu X, McLaughlin NB, Wang G (2011) Carbon Accumulation in Temperate Wetlands of Sanjiang Plain, Northeast China. Soil Sci Soc Am J 75:2386. https://doi.org/10.2136/sssaj2011.0157

Bao K, Wang G, Xing W, Shen J (2015) Accumulation of organic carbon over the past 200 years in alpine peatlands, northeast China. Environ Earth Sci 73:7489–7503

Beilman DW, MacDonald GM, Smith LC, Reimer PJ (2009) Carbon accumulation in peatlands of West Siberia over the last 2000 years. Glob Biogeochem Cycles 23:1–12

Breiman L (2001) Random forests. Mach Learn 45:5–32. https://doi.org/10.1023/a:1010933404324

Chambers FM, Beilman D, Yu Z (2011) Methods for determining peat humification and for quantifying peat bulk density, organic matter and carbon content for palaeostudies of climate and peatland carbon dynamics. Mires Peat 7:1–10

Charman DJ, Beilman DW, Blaauw M, Booth RK, Brewer S, Chambers FM et al (2013) Climate-related changes in peatland carbon accumulation during the last millennium. Biogeosciences 10:929–944. https://doi.org/10.5194/bg-10-929-2013

Christiansen B, Charpentier Ljungqvist F (2012) The extra-tropical Northern Hemisphere temperature in the last two millennia: reconstructions of low-frequency variability. Clim Past 8:765–786

Clymo R (1984) The limits to peat bog growth. Philos Trans R S Lond B Biol Sci 303:605–654

Couˆteaux M-M, Bottner P, Berg B (1995) Litter decomposition, climate and liter quality. Trends Ecol Evol 10:63–66. https://doi.org/10.1016/S0169-5347(00)88978-8

Coulson J, Butterfield J (1978) An investigation of the biotic factors determining the rates of plant decomposition on blanket bog. J Ecol 66:631–650

Davidson EA, Trumbore SE, Amundson R (2000) Soil warming and organic carbon content. Nature 408:789–790

Dong B, Sutton RT, Shaffrey L (2016) Understanding the rapid summer warming and changes in temperature extremes since the mid-1990s over Western Europe. Clim Dyn 48:1–18

Ekwurzel B, Boneham J, Dalton M, Heede R, Mera R, Allen M et al (2017) The rise in global atmospheric CO2, surface temperature, and sea level from emissions traced to major carbon producers. Clim Change 144:579–590

Fang J, Piao S, Field CB, Pan Y, Guo Q, Zhou L et al (2003) Increasing net primary production in China from 1982 to 1999. Front Ecol Environ 1:293–297

Gallego-Sala AV, Charman DJ, Brewer S, Page SE, Prentice IC, Friedlingstein P et al (2018) Latitudinal limits to the predicted increase of the peatland carbon sink with warming. Nat Clim Change 8:907–913. https://doi.org/10.1038/s41558-018-0271-1

Gao J, Ouyang H, Wang G, Xu X (2010) Recent peat accumulation rates in Zoige Peatlands, Eastern Tibet, Inferred by Pb-210 and Cs-137 Radiometric Techniques. In: Yang Z, Chen B (eds) International Conference on Ecological Informatics and Ecosystem Conservation, pp 1927–1933

Gorham E (1991) Northern peatlands: role in the carbon cycle and probable responses to climatic warming. Ecol Appl 1:182–195

Hansen J, Sato M, Ruedy R, Lo K, Lea DW, Medina-Elizade M (2006) Global temperature change. Proc Natl Acad Sci 103:14288–14293

Hastie T, Tibshirani R (1986) Generalized additive models. Stat Sci 1:297–318

Hausfather Z, Cowtan K, Clarke DC, Jacobs P, Richardson M, Rohde R (2017) Assessing recent warming using instrumentally homogeneous sea surface temperature records. Sci Adv 3:e1601207

Hobbie SE (1996) Temperature and plant species control over litter decomposition in Alaskan tundra. Ecol Monogr 66:503–522

Karl TR, Arguez A, Huang B, Lawrimore JH, McMahon JR, Menne MJ et al (2015) Possible artifacts of data biases in the recent global surface warming hiatus. Science 348:1469–1472
Klein ES, Yu Z, Booth RK (2013) Recent increase in peatland carbon accumulation in a thermokarst lake basin in southwestern Alaska. Palaeogeogr Palaeoclimatol Palaeoecol 392:186–195. https://doi.org/10.1016/j.palaeo.2013.09.009
Laiho R (2006) Decomposition in peatlands: reconciling seemingly contrasting results on the impacts of lowered water levels. Soil Biol Biochem 38:2011–2024
Lieth H (1975) Modeling the primary productivity of the world. In: Lieth H, Whittaker RH (eds) Primary productivity of the biosphere. Springer Berlin Heidelberg, Berlin, pp 237–263
Liu H, Gao C, Wei C, Wang C, Yu X, Wang G (2018) Evaluating the timing of the start of the Anthropocene from Northeast China: applications of stratigraphic indicators. Ecol Ind 84:738–747. https://doi.org/10.1016/j.ecolind.2017.09.040
Ljungqvist FC (2010) A new reconstruction of temperature variability in the extra-tropical Northern Hemisphere during the last two millennia. Geogr Ann Ser A Phys Geogr 92:339–351
Loisel J, Yu Z (2013a) Holocene peatland carbon dynamics in Patagonia. Quat Sci Rev 69:125–141
Loisel J, Yu ZC (2013b) Recent acceleration of carbon accumulation in a boreal peatland, south central Alaska. J Geophys Res Biogeosci 118:41–53. https://doi.org/10.1029/2012jg001978
Loisel J, Yu Z, Beilman DW, Camill P, Alm J, Amesbury MJ et al (2014) A database and synthesis of northern peatland soil properties and Holocene carbon and nitrogen accumulation. Holocene 24:1028–1042
Mäkilä M, Saarnisto M, Kankainen T (2001) Aapa mires as a carbon sink and source during the Holocene. J Ecol 89:589–599
Maltby E, Immirzi P (1993) Carbon dynamics in peatlands and other wetland soils regional and global perspectives. Chemosphere 27:999–1023. https://doi.org/10.1016/0045-6535(93)90065-D
Mann ME, Jones PD (2003) Global surface temperatures over the past two millennia. Geophys Res Lett 30:1820
Mao D, Wang Z, Luo L, Ren C (2012) Integrating AVHRR and MODIS data to monitor NDVI changes and their relationships with climatic parameters in Northeast China. Int J Appl Earth Obs Geoinform 18:528–536
Nemani RR, Keeling CD, Hashimoto H, Jolly WM, Piper SC, Tucker CJ et al (2003) Climate-driven increases in global terrestrial net primary production from 1982 to 1999. Science 300:1560–1563
Niu ZG, Zhang HY, Wang XW, Yao WB, Zhou DM, Zhao KY et al (2012) Mapping wetland changes in China between 1978 and 2008. Sci Bull 57:2813–2823
Ridgeway G (2007) Generalized boosted models: a guide to the gbm package. Update 1:2007
Song Y, Zou Y, Wang G, Yu X (2017) Altered soil carbon and nitrogen cycles due to the freeze-thaw effect: a meta-analysis. Soil Biol Biochem 109:35–49. https://doi.org/10.1016/j.soilbio.2017.01.020
State Forestry Administration (2014) The second national wetland resources survey 2009–2013, Beijing, 2014
Stelling JM, Yu Z, Loisel J, Beilman DW (2018) Peatbank response to late Holocene temperature and hydroclimate change in the western Antarctic Peninsula. Quat Sci Rev 188:77–89. https://doi.org/10.1016/j.quascirev.2017.10.033
Stocker BD, Yu Z, Massa C, Joos F (2017) Holocene peatland and ice-core data constraints on the timing and magnitude of CO2 emissions from past land use. Proc Natl Acad Sci USA 114:1492
Straková P, Penttilä T, Laine J, Laiho R (2012) Disentangling direct and indirect effects of water table drawdown on above- and belowground plant litter decomposition: consequences for accumulation of organic matter in boreal peatlands. Glob Change Biol 18:322–335. https://doi.org/10.1111/j.1365-2486.2011.02503.x
Sullivan PF, Arens SJT, Chimner RA, Welker JM (2008) Temperature and microtopography interact to control carbon cycling in a high arctic fen. Ecosystems 11:61–76. https://doi.org/10.1007/s10021-007-9107-y
Tolonen K, Turunen J (1996) Accumulation rates of carbon in mires in Finland and implications for climate change. The Holocene 6:171–178
Ukonmaanaho L, Nieminen TM, Rausch N, Cheburkin A, Le Roux G, Shotyk W (2006) Recent organic matter accumulation in relation to some climatic factors in ombrotrophic peat bogs near heavy metal emission sources in Finland. Glob Planet Change 53:259–268. https://doi.org/10.1016/j.gloplacha.2006.03.008
Van Cleef DJ (1994) Determination of 226Ra in soil using 214Pb and 214Bi immediately after sampling. Health Phys 67:288–289
Wang L, Wu Z, He H, Wang F, Du H, Zong S (2017) Changes in start, end, and length of frost-free season across Northeast China. Int J Climatol 37:271–283
Xing W, Bao K, Gallego-Sala AV, Charman DJ, Zhang Z, Gao C et al (2015) Climate controls on carbon accumulation in peatlands of Northeast China. Quat Sci Rev 115:78–88. https://doi.org/10.1016/j.quascirev.2015.03.005
Yang B, Braeuning A, Johnson KR, Yafeng S (2002) General characteristics of temperature variation in China during the last two millennia. Geophys Res Lett 29:38-1–38-4
Yu Z (2006) Holocene carbon accumulation of fen peatlands in boreal western Canada: a complex ecosystem response to climate variation and disturbance. Ecosystems 9:1278–1288
Yu Z (2012) Northern peatland carbon stocks and dynamics: a review. Biogeosciences 9:4071–4085
Yu Z, Vitt D, Campbell C, Campbell I (2000) Pattern and processes of peat accumulation in continental rich fens: hypothesis and preliminary results. In: Proceedings of the 11th international peat congress, Quebec City, Quebec, Canada, 2000, pp 208–215
Yu Z, Campbell ID, Campbell C, Vitt DH, Bond GC, Apps MJ (2003a) Carbon sequestration in western Canadian peat highly sensitive to Holocene wet-dry climate cycles at millennial timescales. Holocene 13:801–808
Yu Z, Vitt DH, Campbell ID, Apps MJ (2003b) Understanding Holocene peat accumulation pattern of continental fens in western Canada. Can J Bot 81:267–282

**Publisher's Note** Springer Nature remains neutral with regard to jurisdictional claims in published maps and institutional affiliations.